ENHANCED DIAPYCNAL MIXING DURING INTERMEDIARY FLUSHING OF A DEEP SILL FJORD

Linders[1] T., L. Arneborg[1], V. Fiekas[2], M. Knoll[2], H. Prandke[3]

[1] University of Gothenburg, Sweden
[2] FWG, Kiel, Germany
[3] ISW Wassermesstechnik, Petersdorff, Germany

Background

In deep fjords, the flushing of layers above sill level is often dominated by intermediary circulation caused by coastal density field fluctuations, rather than by estuarine circulation and tidal exchanges.

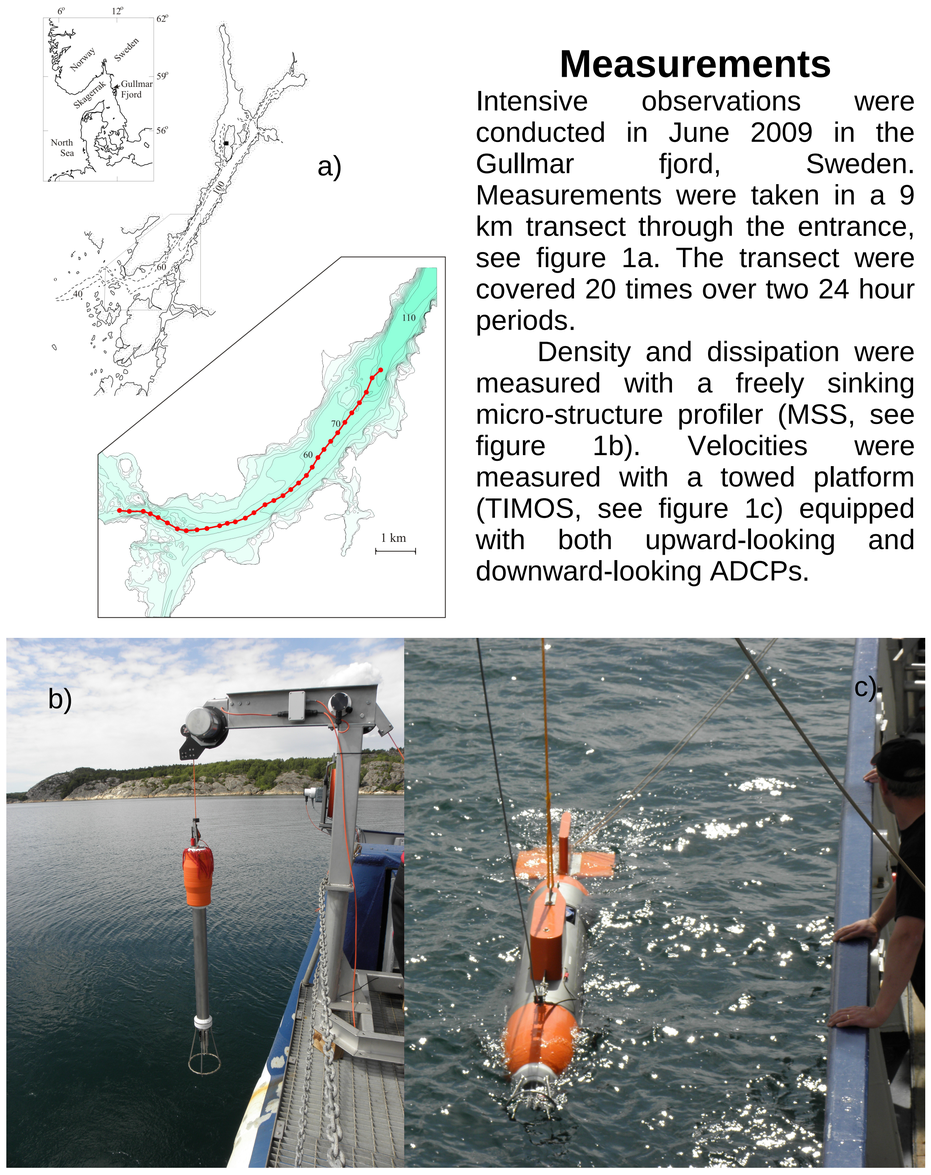

Measurements

Intensive observations were conducted in June 2009 in the Gullmar fjord, Sweden. Measurements were taken in a 9 km transect through the entrance, see figure 1a. The transect were covered 20 times over two 24 hour periods.

Density and dissipation were measured with a freely sinking micro-structure profiler (MSS, see figure 1b). Velocities were measured with a towed platform (TIMOS, see figure 1c) equipped with both upward-looking and downward-looking ADCPs.

Figure 1. Measurements. a) Map showing the Gulmar fjord. The red line with dots indicate profiler casts from ”leg 9”. b) The freely sinking profiler MSS. c) The towed platform TIMOS.

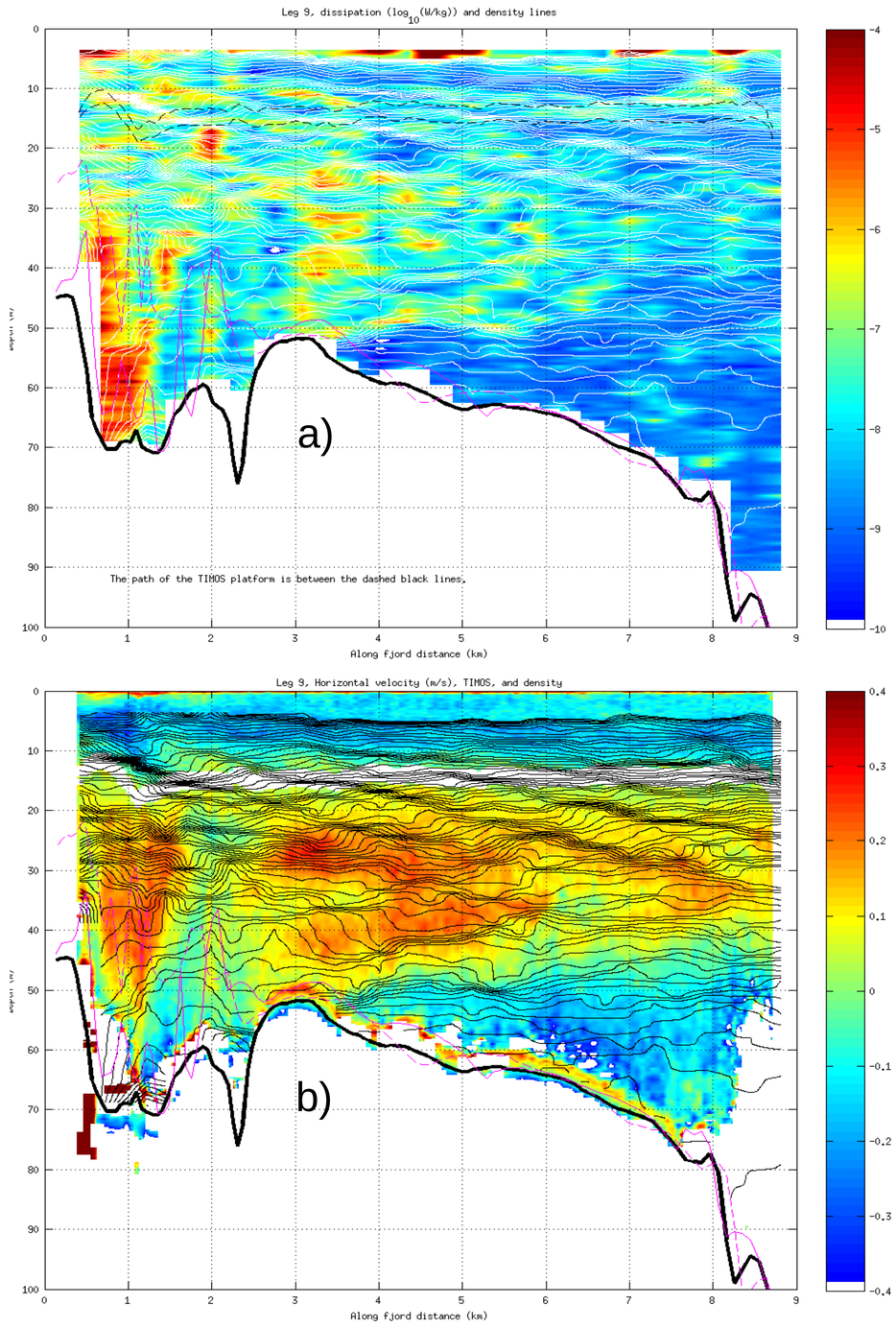

Figure 2. Data from ”leg 9” of the transect. a) Dissipation of turbulent kinetic energy. b) Horizontal along-fjord velocity (positive from left to right). Density lines are included in both panels.

Result

A flushing event occurred during one of the 24 h periods, with strong inflow at intermediate levels. This coincided with enhanced dissipation rates at the levels of inflow in a wedge extending 6 km into the fjord, see figure 2.

The density and dissipation rate fields reveal non-linear, oblique internal wave beams with typical horizontal length scales from 0.3 to 3 km. The beams extend from the bottom and from the halocline near the entrance towards the center of the inflowing layer, bounding the wedge of enhanced dissipation, see figure 2.

Data from the entire 24 h period show that the dissipation rate has a rather consistent Richardson number dependency, with higher dissipation rates for lower Richardson numbers, see figures 3b and 4a. However, for buoyancy-frequency and shear the picture is little bit more mixed, see figure 3b and c. Dissipation rates appear to be independent of the shear – for values of shear squared below 10^{-4} s^{-2}.

Discussion

Increasing dissipation rates with decreasing Richardson numbers correspond to what one would expect intuitively. However, one would expect practically zero dissipation rates for Ri > 1/4. The reason for the high background dissipation rates at low shear and high buoyancy frequency may be lingering turbulence and small (< 4 m) vertical scale internal wave breaking. The background dissipation rates in the wedge are dramatically larger during the inflow, indicating sources related to the oblique waves and/or the hydraulic jump at the sill.

Our shear and buoyancy frequency dependency reminds of the one of Gregg (1989), and is very different from the continental shelf parametrization obtained by MacKinnon and Gregg (2003). The latter predicts increasing dissipation rates with increasing buoyancy frequency. The Gregg (1989) scaling is based on small-scale waves interacting with larger scale shear transferring energy towards smaller scales. This may be what happens with the small-scale oblique waves interacting with the large scale shear in the inflow.

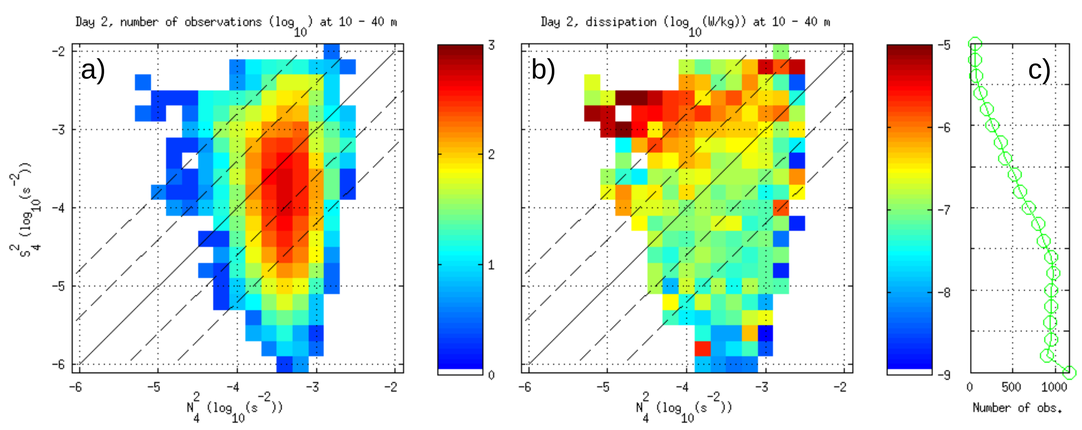

Figure 3. Data from one 24 hour period, ”day 2”. a) Distribution of observations in N^2-S^2-space. b) Dissipation in N^2-S^2-space. c) Distribution of observation in dissipation bins. Thin solid line show *Ri*=1, thin dashed lines show *Ri*=1/16, *Ri*=1/4,*Ri*=4 and *Ri*=16.

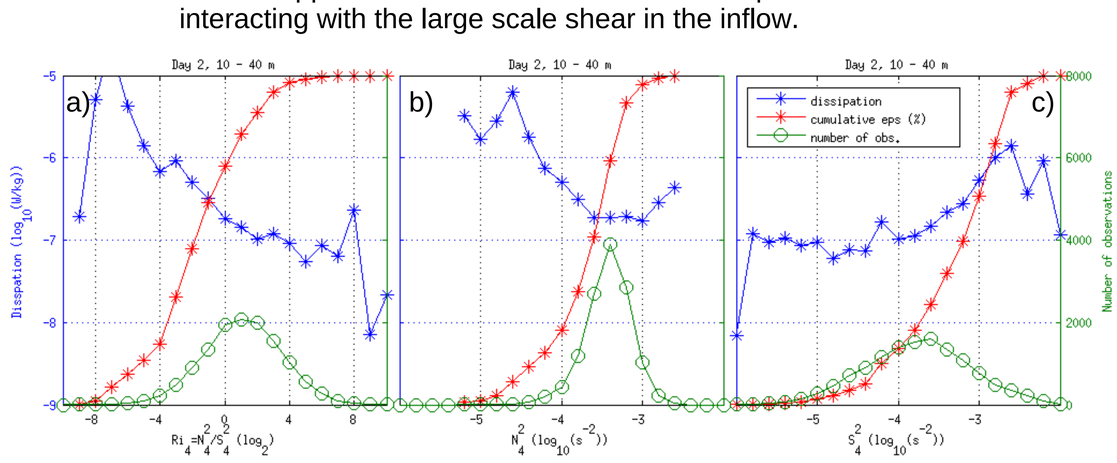

Figure 4. Data from one 24 hour period, ”day 2”. Dissipation and distribution of observations plotted against a) Richardson number, b) Buoyancy frequency squared and c) shear squared. Also plotted is the distribution of cumulative of dissipation, with 0 % at the bottom and 100 % at the top of each panel.